

# Activation energy of poly(methyl methacrylate) from rheometry and polymer welding

Mathias Vinggaard · Jesper de Claville Christiansen

Received: 26 September 2010/Accepted: 5 February 2011/Published online: 17 February 2011  
© Springer Science+Business Media, LLC 2011

**Abstract** In this article, activation energies for a poly(methyl methacrylate) material were determined by shear rheometry and by bond strength in welding. Functions for temperature dependency of viscosity and for bond strength, depending on time and temperature, were found. These functions were fitted to measurements from shear rheometry between 230 and 270 °C and from strength of lap-shear joints welded from 105 to 130 °C, where by values of activation energies were found. It was found that bonding pressure was less than significant. Despite experimental differences, there was good correlation with data from literature for each method as well as for temperature dependency.

## Introduction

Activation energy,  $E_a$ , affect rheometric properties and diffusion, which can be correlated to strength of a polymer weld, e.g. in joining of polymers and in weld-lines from plastics moulding. However, measurement methods often influence results and this was also part of the conclusion by Boiko and Lyngaae-Jørgensen [1], when they compared values for  $E_a$  from fracture energy and fracture strength, i.e. bond strength.

In this article, two even more distinct methods were employed in determining values of activation energy. Shear rheometry is a standard technique to determine viscosity and  $E_a$  can be calculated by fitting a function to a suitable

data set. Polymer welding is a common method for joining, but it is not standard for measuring material properties. A function for macroscopic strength based on molecular diffusion was fitted to the data for strength, thereby making it possible to determine a value for  $E_a$ .

## Molecular chain dynamics

Bonding can be divided into several stages. Initially, the *approach* of the surfaces is when microscopic deformation is taking place, so that two pieces of polymer come in contact with each other. *Wetting* can often be assumed instantaneous, but only when wetting has taken place can the strength development in the next phases begin. The phases *diffusion* and *randomisation* are where molecular dynamics are governing the forming of bond strength [2].

The diffusion and randomisation of the chain configuration will cause some of the molecular chains to move, so that they lie across the interface between the two polymer pieces. After some time so many molecules will lie across the interface, that it is indistinguishable from the bulk materials. The bond strength between two surfaces of polymer is almost solely determined by the molecular chain configuration and wetting can often be neglected.

## Bond strength

In fracture of glassy polymers, the molecular chains are either broken or they are pulled out. Both things may happen in combination at the same macroscopic fracture. By broken as well as by pulled-out chains, the strength,  $\sigma$ , is proportional to diffusion depth normal to the interface plane,  $X(t)$ .  $X(t)$  will increase, depending on time, temperature and molecular properties, caused by contributions from molecular dynamics at several time scales. Wool [2]

M. Vinggaard · J. de Claville Christiansen (✉)  
Department of Mechanical and Manufacturing Engineering,  
Aalborg University, Fibigerstræde 16, 9200 Aalborg Ø,  
Denmark  
e-mail: jc@m-tech.aau.dk

gave an example of molecular time scales for polystyrene which at 118 °C with a molecular weight of 245 kg/mol has a Rouse relaxation time,  $\tau_{\text{Rouse}}$ , around 21 min and a reptation time,  $\tau_{\text{rep}}$ , of about 1860 min.

The time scale  $\tau_{\text{Rouse}} < t < \tau_{\text{rep}}$  is important for welding, and that  $X(t) \propto t^{1/4}$  is well known. However, the  $t^{1/4}$  correlation only arises as time approaches  $\tau_{\text{rep}}$ , where the contribution from Rouse relaxation loses importance [2].

The diffusion coefficient,  $D$ , can be written as in Eq. 1 [3], where  $\rho$  is the density,  $R$  is the gas constant,  $T$  is the absolute temperature,  $R_g$  is the radius of gyration,  $M$  is the molecular weight,  $M_c$  is the critical molecular weight, and  $\eta_{0,M_c}$  is zero shear viscosity at  $M_c$ .

$$D = \left( \frac{\rho RT}{270} \right) \left( \frac{M_c}{M} \right)^2 \left( \frac{R_g^2}{M} \right) \left( \frac{1}{\eta_{0,M_c}} \right) \quad (1)$$

The zero shear viscosity at critical molecular weight,  $\eta_{0,M_c}$ , depends on temperature and can be calculated according to Eq. 2 [3], where  $c$  is a material constant and  $E_a$  activation energy. Boiko and Lyngaae-Jørgensen [1] explained activation energy as the energy needed to overcome the contact interface.

$$\eta_{0,M_c} = c \exp \left( \frac{E_a}{RT} \right) \quad (2)$$

Equation 1 can be simplified, when it is applied for the same material at various temperatures. The first terms vary little, and the last term containing  $\eta_{0,M_c}$ , can vary several orders of magnitude within normal temperatures of application. Thus,  $D$  can be described by Eq. 3 [4] and its approximation [1] containing the constant  $c'$ .

$$D = T \frac{1}{c} \exp \left( \frac{-E_a}{RT} \right) \approx c' \exp \left( \frac{-E_a}{RT} \right) \quad (3)$$

Equation 4 describes the diffused length normal to the interface for times shorter than the reptation time [1].  $X(t)$  is the diffusion length,  $a$  is a constant and  $t$  is contact time.

$$X(t) = a(2Dt)^{1/4} \quad (4)$$

The proportionality of bond strength,  $\sigma_{\text{bond}}$ , to the diffusion length implies Eq. 5 [1], where in the following  $b$ ,  $b'$  and  $b''$  are constants.

$$\sigma_{\text{bond}} = b(2Dt)^{1/4} \quad (5)$$

Equations 5 and 3 lead to an expression for the bond strength as function of time and temperature, as written in Eq. 6 [4].

$$\sigma_{\text{bond}} = b'T^{1/4} \exp \left( \frac{-E_a}{4RT} \right) t^{1/4} \quad (6)$$

Based on the approximation in Eq. 3, the expression for bond strength can be written as in Eq. 7 [1].

$$\sigma_{\text{bond}} = b'' \exp \left( \frac{-E_a}{4RT} \right) t^{1/4} \quad (7)$$

Hence, it can be seen that  $E_a$  in the expression for bond strength originates from the temperature dependency of a specific viscosity value.

## Experiments from literature

Jud et al. [5] welded and healed poly(methyl methacrylate), i.e. PMMA, samples at temperatures from glass transition temperature,  $T_g$ , +2 K to  $T_g$  + 15 K at approximate contact times,  $t$ , from a few seconds to 1000 min. They found that fracture toughness was proportional to  $t^{1/4}$ , implying  $\sigma_{\text{bond}} \propto t^{1/4}$ , and that the diffusion coefficient expressed Arrhenius behaviour. Shim and Kim [6] welded lap-shear joints of acrylonitrile-butadiene-styrene at  $T_g$  + 50 K to  $T_g$  + 200 K with contact times from 10 to 60 min, and they found that  $\sigma_{\text{bond}} \propto t^{1/4}$ . Hence, both references found that results from bonding of amorphous polymers above  $T_g$  was in agreement with Eq. 7.

A small amount of pressure is necessary to ensure wetting contact, but increasing pressure further than this can influence the bonding process. During welding of polystyrene, PS, at 115 °C for 30 min, a pressure increase from 0.3 to 2 MPa reduced fracture energy with about 15 % [2]. When experimenting with PS above  $T_g$ , it has been found that rising pressure above 50 MPa increases viscosity and decreases diffusion [7].

Guérin et al. [8] did annealing of PS for 60 min at  $T_g$  + 10 °C to remove residual stresses before bonding double cantilever beams.

Bond strength of lap-shear joints in PS welded above  $T_g$  showed no variation with cross-head speeds between 0.13 and 12.5 mm/min [9]. Kim and Shim [6] experimented with lap-shear joints consisting of 3-mm thick strips and assumed pure shear. References [8, 9] and [1] investigated lap-shear joints of strips with 0.1 mm thickness, where they also assumed pure shear in the joint.

## Activation energy from rheometry

The empirical Cox–Merz rule states that complex viscosity,  $\eta^*$ , as a function of angular frequency,  $\omega$ , can be assumed equal to viscosity,  $\eta$ , as function of shear rate  $\dot{\gamma}$ , as in Eq. 8 [10, 11]. Sui and McKenna [12] investigated a polybutadiene solution in rheometry and found that any deviations from the Cox–Merz rule were caused by edge fracture. In this article, the Cox–Merz rule was applied to data from oscillatory shear rheometry.

$$|\eta^*(\omega)| = \eta(\dot{\gamma})|_{\dot{\gamma}=\omega} \quad (8)$$

Temperature dependency of viscosity can be modelled by an Arrhenius expression, as in Eq. 9, when

$T > T_g + 100^\circ\text{C}$  [13–15]. Here,  $E_a$  implies an energy barrier which has to be overcome before flow can take place [16].

$$\eta = A \exp\left(\frac{E_a}{RT}\right) \quad (9)$$

From two viscosities,  $\eta_1$  and  $\eta_2$ , measured at two temperatures,  $T_1$  and  $T_2$ , respectively, and at constant shear rate the activation energy can be determined from Eq. 10 [1, 17].

$$\ln\left(\frac{\eta_1}{\eta_2}\right) = \frac{E_a}{R} \left( \frac{1}{T_1} - \frac{1}{T_2} \right) \quad (10)$$

For linear amorphous polymers in the region of non-Newtonian flow,  $E_a$  decreases with shear rate [16, 18]. By calculating  $E_a$  from zero shear viscosity of the modified Carreau expression in Eq. 11 [11], the effect of shear rate can be eliminated.  $\eta_0$  is zero shear viscosity,  $\dot{\gamma}$  is shear rate and  $\tau^*$  as well as  $n$  are material constants.

$$\eta = \frac{\eta_0}{(1 + \eta_0 \dot{\gamma} / \tau^*)^{1-n}} \quad (11)$$

Berry and Fox [19] studied  $E_a$  in connection with temperature dependency of viscosity, and they found that it decreases with temperature. The correlation can be described by Eq. 12, where  $\alpha$  and  $T_0$  are empirical material constants from the Vogel–Fulcher–Tammann equation [19]. According to Miller [20],  $T_0$  is the temperature at which the free volume becomes zero, and  $\alpha$  is a kinetic parameter related to barriers against rotation of bonds in the main chain, with no connection to any expansion coefficients. Cisse et al. [21] studied diffusion in PMMA and found that activation energy was constant, but the temperature range of  $53^\circ\text{C}$  may have been too narrow to allow measurement of any changes. Grewell and Benatar [22] proposed an exponential function for  $E_a$  decreasing temperature, but in this work Eq. 12, probably a better description, will be applied.

$$E_a = R / (\alpha(1 - T_0/T)^2) \quad (12)$$

Around  $T_g + 150^\circ\text{C}$  [16],  $E_a$  approaches a constant value,  $E_a^*$ , according to the Eq. 13, which depends on  $\alpha_l$ , the volume expansion coefficient above  $T_g$ , as well as  $T_g$ . The Simha–Boyer expression,  $\alpha_l T_g = 0.164$ , was by Wang and Porter [16] found to provide approximate correlation with  $E_a^*$ .

$$E_a^* = \frac{R}{\alpha_l} \frac{(T_g + 150)^2}{(0.23T_g + 150)^2} \quad (13)$$

No examples from literature have been found with quantitative comparison between activation energy from temperature dependency of viscosity and from bond strength. Boiko and Lyngaae-Jørgensen [1] compared

values for  $E_a$  obtained from fracture energy in a peel test and bond strength of a lap-shear joint, and they concluded that values were *strongly dependent* on the measurement method. Thus, deviations were also expected when comparing  $E_a$  from rheometry and from welding in the work described in this article.

## Experimental

The chosen PMMA material, extruded sheets of PLEXIGLAS® 7H from Evonik Röhm GmbH, had a nominal average molecular weight,  $M_w$ , of 150 kg/mol. Katsikis [23] mentioned that PLEXIGLAS® 7H is 70% syndiotactic and 30% atactic and that  $M_w$  has a value of 141 kg/mol.

### Preparation of PMMA strips

In each welding, a pair of strips were welded together to form a lap-shear joint, which is sketched in Fig. 1.

The choice of strip thickness was a compromise between a thin strip for faster cooling after welding, and a thick strip to allow for experiments with a higher bond strength before strip fracture. Each strip with a thickness of 1.5 mm, was cut to dimensions  $25 \times 50$  mm. Prior to annealing, the strips were wiped with ethanol to ensure consistent clean surfaces. Annealing was carried out to remove residual stress and thereby to minimise warping during welding. The annealing in this experiment took place around a lower bound value for  $T_g$ , i.e.  $105^\circ\text{C}$ , for 60 min, and the samples were then being cooled down to around  $60^\circ\text{C}$  over 2 h. Prior to pressing, a pair of strips at room temperature were placed in a positioning frame and heated in an oven for 15 min to ensure homogeneous temperatures.

### Process steps in welding

Welding was carried out with two heated stamps in an Instron 5568 tensile testing machine. The positioning frame was a spring loaded design which, before welding, enabled positioning of one PMMA strip on the bottom stamp and an identical strip on the top stamp with a specified overlap. The steps of the process were as described in the following.

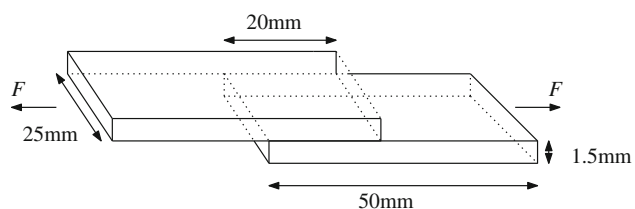


**Fig. 1** A sample, i.e. a lap-shear joint, made from two strips joined by welding

Heating and positioning of strips: (1) the two stamps were held together and the top stamp was raised when the stamp temperatures, i.e. bonding temperature  $T_b$ , had stabilised around  $\pm 1$  °C. (2) One strip was placed on the bottom stamp, then the preheated positioning frame was placed onto it with the second strip on the top. (3) A weak adhesive was applied to the top strip. (4) The top stamp was lowered until it was in contact with the top strip. (5) The top stamp was raised, and the adhesive ensured the top strip stucked to it. (6) The positioning frame was removed, leaving one strip on the bottom stamp, while the other strip was glued to the top stamp.

*Bonding:* (7) The top stamp was lowered until the two strips were pressed together with the specified bonding pressure,  $P_b$ . (8) The position of the top stamp was held constant for the specified bonding time,  $t_b$ , and welding was taking place.

*Removal and cooling of sample:* (9) The top stamp was raised, and the welded lap-shear joint stucked to the steel surface of the top stamp. (10) The sample was removed and left to cool.

The extension of the tensile testing machine was held constant, which caused a decrease of the force because the melted plastic flowed due to slight squeezing by the stamps. The pressure transducer was calibrated between each heating and pressing.

#### Experimental design

Bond strength,  $\sigma_{\text{bond}}$ , was assumed as a function of the three process parameters bonding temperature,  $T_b$ , bonding time,  $t_b$  and bonding pressure,  $P_b$ . The experimental design was a spherical central composite design with 19 runs based on a  $2^3$  factorial design, i.e. eight runs, with six axial runs added for expected non-linearity plus five centre runs. The lower limit for the bonding temperature,  $T_b$ , was set to  $T_g$ , and the upper limit was around the temperature where the strips became too liquid for handling. Bonding time,  $t_b$ , was not investigated above 120 s. The lower limit for bonding pressure,  $P_b$ , was set to ensure wetting in the overlapping area between the strips. The upper limit was where the strips would be squeezed too far out shape from the lap-shear joint. Thus, the nominal intervals for the three process parameters became as follows:  $T_b = [105; 130]$  °C,  $t_b = [0; 120]$  s and  $P_b = [0.4; 4]$  MPa.

#### Bonded area

For calculation of the real bonding pressure as well as the bond strength, the real area of overlap was measured. Each welded sample was submerged in a dark contrast liquid with a white background, whereby the overlapping area presented itself as bright in digital image analysis.

#### Bond strength

The bond strength was measured in an Instron 5568 tensile testing machine, where the cross-head speed was set to 1.3 mm/min and pure shear was assumed.

#### Oscillatory shear rheometry

Cone-and-plate oscillatory shear rheometry was carried out with an Anton Paar, Paar Physica MCR 500 rheometer, where the cone had a diameter of 25 mm and a 2° angle. The measurements were carried out at 230, 250 and 270 °C with frequency sweeps from 628 1/s in oscillatory mode. Recordings were halted at 0.06 1/s or above if the viscosity decreased, due to molecular degrading, edge fracture or another error.

## Results and discussion

Two methods were employed to determine values for activation energy; bond strength from welding and temperature dependency of viscosity from oscillatory rheometry.

#### Bond strength from welding

Errors in time, temperature or pressure could influence apparent bond strength in both directions, but minor distortions during welding or misalignment in tensile testing would most likely lead to reduced apparent bond strength. By fitting Eq. 7 to the data, it was found that the largest negative residual for a certain point was more than 1.5 times the second largest value. Thus, the relevant point, one of the two points at  $(T_b, t_b) = (398 \text{ K}, 25.4 \text{ s})$ , was considered an outlier and omitted from the following investigations of the 18 remaining points.

When fitting Eq. 7 with a linear pressure term, bonding pressure during welding proved to be insignificant with a  $p$  value of 0.25 at a significance level of 0.90. This indicates, that there has been wetting in the whole overlapping area, even for the low values of bonding pressure. And as expected for these relatively low bonding pressures, even the high values of  $P_b$  have not slowed down diffusion.

Figure 2 shows an overview of the measurements and the fitted function in Eq. 7. The nonlinear increase of bond strength with bonding temperature and bonding time can be immediately observed. The five centre points at the nominal values  $(T_b, t_b, P_b) = (390.5 \text{ K}, 60 \text{ s}, 2.2 \text{ MPa})$  are indistinguishable from the two points from the variations of the third and insignificant process parameter, bonding pressure. Also, due to variants with different bonding pressure, there are pairs of points visible at 25 and 95 s.

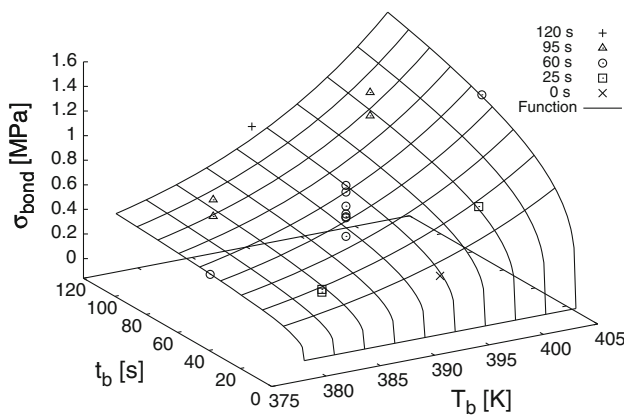


**Fig. 2** Bond strength,  $\sigma_{\text{bond}}$ , plotted against the central composite design of bonding temperature,  $T_b$ , and bonding time,  $t_b$ , while there is no axis for bonding pressure. Measurements are plotted with symbols according to bonding time: 0, 25, 60, 95 or 120 s. The fitted function in Eq. 7, where  $E_a$  became 320 kJ/mol, is shown as well

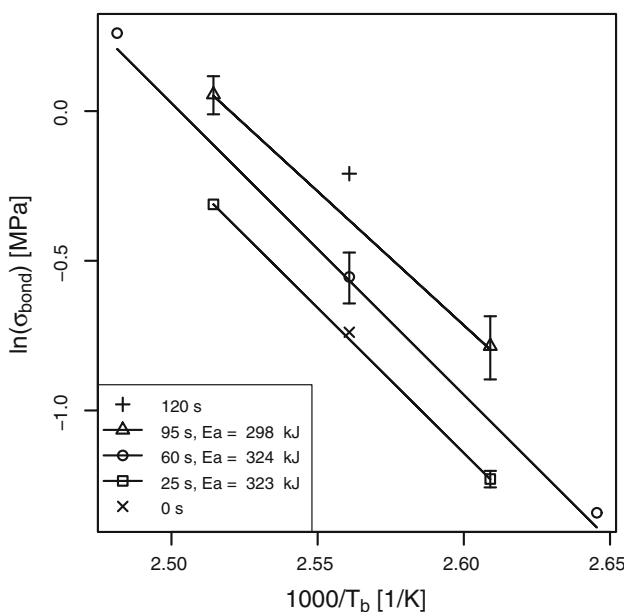


**Fig. 3** Logarithm of  $\sigma_{\text{bond}}$  plotted against  $1000/T_b$ . Points indicate mean, and where more than one measurement was available, error bars indicate mean  $\pm$  standard deviation of the mean. The local values of  $E_a$ , determined for a check of data, were based only on data for the indicated bonding time

Figure 3 shows an Arrhenius plot of the bond strength means, with the individual points in Fig. 2, against bonding temperature. For  $t_b$  equal to 60 s, standard deviation of the mean was determined from seven replications, while standard deviations of the mean at 25 and 95 s were found from two replications. When fitting Eq. 7 to data separately at three levels of bonding time, 25, 60 and 95 s, deviations from the  $E_a$  for all bonding times were 0.8, 1 and −7%, respectively. This, as expected, ruled out correlation between  $E_a$  and  $t_b$ .

For the further investigations, the value of  $E_a$  at the average temperature of 390.5 K was determined to 320 kJ/mol from a fit of Eq. 7 to all 18 points, shown in Fig. 2.

#### Oscillatory shear rheometry

Viscosity was measured at 230, 250 and 270 °C which allowed the calculation of  $E_a$ , for each of the two temperature intervals, i.e. average temperature 240 and 260 °C, i.e. 513–533 K. The viscosity data points are shown in Fig. 4.

Figure 5 is a plot of  $\ln(\eta)$  against  $1000/T$ , where the slope for Eq. 9 becomes  $E_a/(1000 R)$ . The purpose of the plot is to compare how well measured and extrapolated viscosities fit the theory of  $E_a$  decreasing with temperature. The viscosities at the lowest shear rate with data for all three temperatures, i.e. 1.31 1/s, as well as viscosities at zero shear rate, from extrapolation of Eq. 11, are plotted. For the measured data, the slope and thereby also  $E_a$  is larger at the high temperatures, 1.84–1.91 1/K, than at the low temperatures, 1.91–1.99 1/K. This is against established theory wherefore only the extrapolated data, where the slope, including  $E_a$ , is close to constant, will be explored further in this article. This plot corresponds to Fig. 3 in Ref. [6] and to Fig. 1 in Ref. [16].

#### $E_a$ from welding and from rheometry

The purpose of Fig. 6 is to compare values for activation energy,  $E_a$ , at different temperatures. The three lines illustrate Eq. 12 with the constants in Table 1.

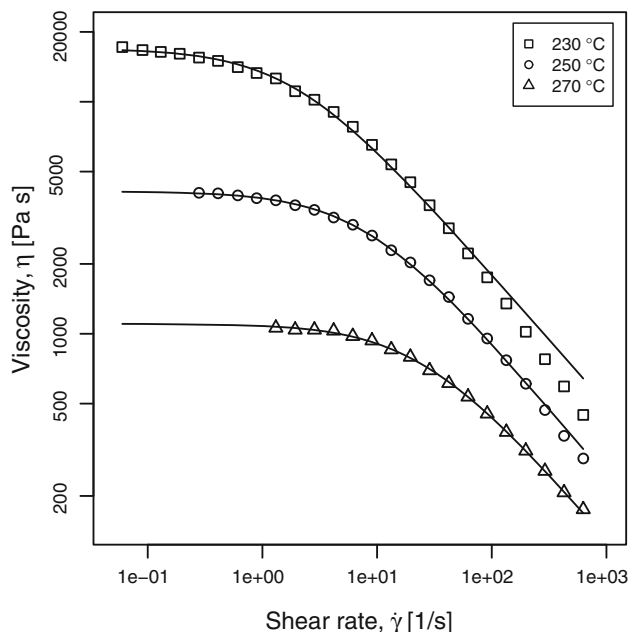


**Fig. 4** Double logarithmic plot of viscosity,  $\eta$ , as function of shear rate,  $\dot{\gamma}$  at three temperatures. The three lines represent fitted functions according to Eq. 11

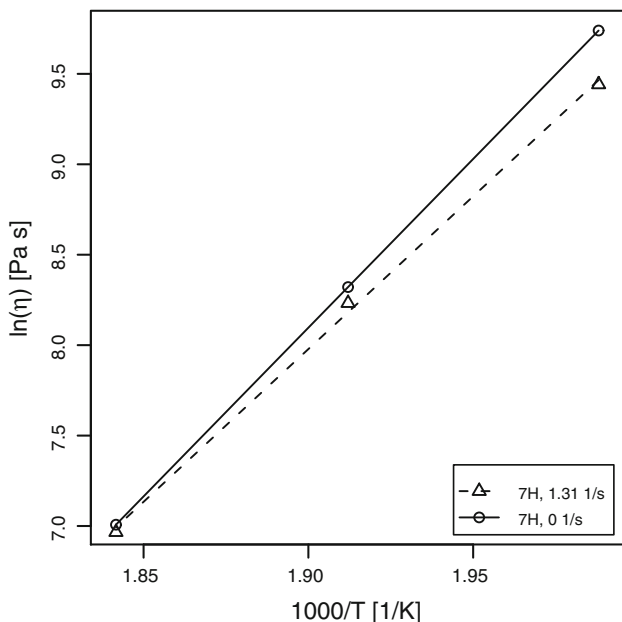


**Fig. 5** Measured data,  $\ln(\dot{\eta} = 1.31 \text{ 1/s})$ , and extrapolated data,  $\ln(\eta_0)$  against  $1000/T$ .  $1000/(230 \text{ }^\circ\text{C})$  equals  $1.99 \text{ 1/K}$ ,  $1000/(250 \text{ }^\circ\text{C})$  is  $1.91 \text{ 1/K}$  and  $1000/(270 \text{ }^\circ\text{C})$  is  $1.84 \text{ 1/K}$ .  $7H$  indicate PLEXIGLAS® 7H. Lines serve only as guides for the eyes: dashed lines for measured data and solid lines for extrapolated data

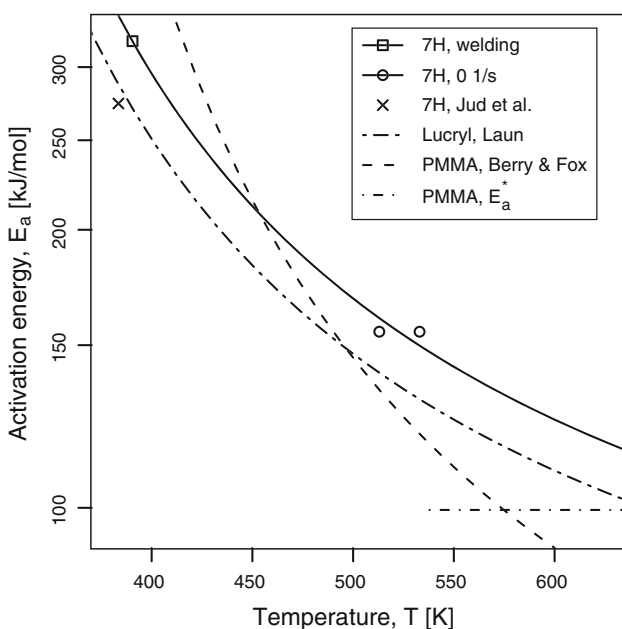


**Fig. 6** Semi-logarithmic plot of activation energies,  $E_a$ , against temperatures determined by different methods. Experiments described in this article are represented by  $7H$ , welding and  $7H$ ,  $0 \text{ 1/s}$  and the solid line fitted to these three points

The point  $7H$ , welding is  $E_a$  of  $320 \text{ kJ/mol}$  found from welded bond strength at an average of  $390.5 \text{ K}$ . The two points  $7H$ ,  $0 \text{ 1/s}$  are  $E_a$  from rheometry. For the two points

**Table 1** Constants of Eq. 12 determined in three of the experiments included Fig. 6

Plot legend	Ref.	$10^4 \times \alpha [\text{1/K}]$	$T_0 (\text{K})$
7H, welding	This	1.93	247
7H, 0 1/s	Work		
Lucryl, Laun	[24]	2.13	242
PMMA, Berry & Fox	[19]	3.88	308

$7H$ ,  $0 \text{ 1/s}$  there is a small decrease of  $E_a$  from average temperature of  $513\text{--}533 \text{ K}$ . The solid line represents a fit of Eq. 12 to the single point  $7H$ , welding and the two points  $7H$ ,  $0 \text{ 1/s}$ .

The single point  $7H$ , *Jud et al.* is the value for  $E_a$  found by *Jud et al.* [5] from experiments with crack healing and welding of compact tension geometries at  $381 \text{ K}$  of PMMA 7H from *Röhm GmbH*, assumed to be the same grade as PLEXIGLAS® 7H, with weight average molecular weight of  $120 \text{ kg/mol}$ . The two  $E_a$  values determined for thermal bonding,  $320 \text{ kJ/kg}$  for  $7H$ , welding and  $274 \text{ kJ/kg}$  for  $7H$ , *Jud et al.*, deviate only around 14% despite the long-time span between the two different experiments on thermal bonding.

*Lucryl, Laun* is data for Lucryl G 77 from BASF, consisting of 95% PMMA by weight and with weight average molecular weight of  $88 \text{ kg/mol}$ , measured by rheometry at temperatures from  $423$  to  $540 \text{ K}$  [24]. The line representing Laun's data is remarkably close to the point found by *Jud et al.* from a different method and a different grade. Data for Lucryl lies below the data for 7H found in this work in the whole temperature interval, i.e. both for welding and rheometry.

The line *PMMA, Berry & Fox* is for PMMA, approximately 75% syndiotactic, based on data from around  $413$  to  $513 \text{ K}$  [19]. However, these constants were described as inaccurate over wide temperature intervals.

As expected, in Table 1 all three fitted  $T_0$  values lie below  $T_g$  of PMMA. When comparing fitted values of  $\alpha$  and  $T_0$  based on this work to those based on the work by Laun [24] they are close, especially when considering that grade, measurement methods and temperature intervals were different. The difference between the line *PMMA, Berry & Fox* and the two other lines is primarily caused by the large relative difference of the  $\alpha$  values. However, the differences between the PMMA grades may be explained not only by differences in PMMA molecules, but also by different fractions of ethyl methacrylate, which is added to most commercial PMMA grades [2].

The line *PMMA,  $E_a^*$*  was drawn according to Eq. 13 with  $T_g$  set to  $388 \text{ K}$  and  $\alpha_f$  found from  $T_g$  in the Simha-Boyer expression. The line *PMMA, Berry & Fox* intersect *PMMA,  $E_a^*$*  at  $T_g + 187 \text{ K}$ , which is above the predicted value of  $T_g$

+ 150 K. The solid line, fitted to 7H, *welding* and 7H, 0 1/s, as well as the dashed line, fitted to *Lucryl*, *Laun*, both intersect  $E_a^*$  at temperatures much larger than  $T_g + 150$  K.

## Conclusion

Activation energy,  $E_a$ , was determined at different temperatures by bond strength of welding, with variations of both time and temperature, and by temperature dependency of viscosity in rheometry.

Zero shear viscosities provided a more correct value of  $E_a$ , which is decreasing with temperature, than viscosities at finite values of shear rate.

The  $E_a$  value found in this work for PMMA 7H by welding of lap-shear joints deviated only 14% from the value found by Jud et al. [5] for welding and healing of a different sample geometry.

Correlation of  $E_a$  with temperature was similar for the two commercial grades, 7H and Lucryl, where difference between the fitted constants were maximum 10%.

Despite the determination of  $E_a$  by different methods, welding and rheometry, there was good correlation between data from literature and data from the experiments described in this article.

**Acknowledgements** The authors gratefully acknowledge the funding from Lego®.

## References

- Boiko YM, Lyngaae-Jørgensen J (2005) Polymer 46(16):6016
- Wool RP (1995) Polymer interfaces: structure and strength. Carl Hanser Verlag, Munich
- Pecorini TJ, Seo KS (1996) Plast Eng 52(6):31
- Cho BR, Kardos JL (1995) J Appl Polym Sci 56(11):1435
- Jud K, Kausch HH, Williams JG (1981) J Mater Sci 16:204. doi: 10.1007/BF00552073
- Shim MJ, Kim SW (1997) Mater Chem Phys 48(1):90
- Chen RS, Hua YS, Huang DY (1999) J Polym Eng 19(6):419
- Guérin G, Mauger F, Prud'homme RE (2003) Polymer 44(24): 7477
- Boiko YM, Prud'homme RE (1998) Macromolecules 31(19): 6620
- Yasuda K, Armstrong RC, Cohen RE (1981) Rheol Acta 20(2): 163
- Hieber CA, Chiang HH (1989) Rheol Acta 28(4):321
- Sui C, McKenna GB (2006) Breakdown of the Cox-Merz rule and instability of polymer solutions in viscometric flows, ANTEC Papers: 2006, Society of Plastics Engineers
- Liu CY, He J, Keunings R, Bailly C (2006) Macromolecules 39(25):8867
- Tanguy PA, Choplin L, Hurez P (1988) Polym Eng Sci 28(8):529
- Mekhilef N, Ait-Kadi A, Ajji A (1995) Polymer 36(10):2033
- Wang JS, Porter RS (1995) Rheol Acta 34(5):496
- Abraham T, Banik K, Karger-Kocsis J (2007) Exp Polym Lett 1(8):519
- Kartsovnik WI, Pelekh VV (2007) Cornell University Library, Ithaca. <http://www.arxiv.org>. arXiv:0707.0789v1. Accessed 30 January 2011
- Berry GC, Fox TG (1968) Adv Polym Sci 5:261
- Miller AA (1969) Macromolecules 2(4):355
- Cisse AL, Grossman E, Sibener SJ (2008) J Phys Chem B 112(24):7166
- Grewell D, Benatar A (2006) Multi physical coupled model: Predictions of healing with microwelding of plastics, ANTEC Papers: 2006, Society of Plastics Engineers
- Katsikis N (2008) Diss Univ Erlangen-Nürnberg
- Laun HM (1998) Pure Appl Chem 70(8):1547